Perturbed-angular-correlation studies of 2^+ levels of even xenon isotopes

D. M. Gordon* and L. S. Eytel†
Rutgers University,‡ New Brunswick, New Jersey 08903

H. deWaard§ and D. E. Murnick¶
Bell Laboratories, Murray Hill, New Jersey 07974
(Received 13 January 1975)

Thin solid xenon targets were prepared by condensing xenon gas on iron at 4.2 K. First 2^+ levels of $^{124-132}$Xe were Coulomb excited and recoil implanted into the polarized iron foils. $B(E2\uparrow)$ values and g factors were determined from excitation and perturbed angular correlation data, respectively, and are in reasonable agreement with collective model calculations. A value for the average hyperfine field on xenon implanted into iron under these experimental conditions was determined to be $H_{\text{eff}} = 1.40 \pm 0.37$ MOe.

[NUCLEAR STRUCTURE $^{124-132}$Xe, 2^+ levels Coulomb excited, 36–42 MeV ^{16}O, $W(\theta)$, deduced $B(E2\uparrow)$, g factors, H_{eff} Xe (Fe).]

I. INTRODUCTION

Heavy-ion Coulomb excitation followed by recoil implantation perturbed angular correlation (IMPAC) measurements have been a productive experimental technique for the study of magnetic moments of 2^+ states of even-even nuclei.[1,2] The major advantages of this method are its versatility, in that any stable isotope can be excited with reasonable cross section, and the highly anisotropic 0-2-0 particle-γ correlation obtained with backscattered spin-zero particles, enhancing sensitivity to small angular shifts. In addition, the large hyperfine magnetic fields effective on impurities at rest in, or recoiling through, ferromagnetic media allow measurements for states living as briefly as 1 psec.

From a nuclear structure standpoint, xenon is especially interesting as there are seven stable even-even isotopes from $^{124}_{54}\text{Xe}_{70}$ to $^{136}_{54}\text{Xe}_{82}$ at a closed neutron shell. First-excited 2^+ state energies smoothly vary from 355 keV to 1.3 MeV. The low-lying level structure is thought to be vibrational, though experimental data are sparse. Previous studies on neighboring isotopes, tellurium[2] ($Z = 52$) and barium[3] ($Z = 56$), yielded 2^+ state magnetic moment values consistent with a simple collective model for those nuclides. It was anomalies in data for the Te isotopes which led to the discovery of the transient magnetic field effect on fast ions in ferromagnetic solids.[4]

In an IMPAC experiment, the measured parameter is an angular shift $\Delta\theta$ of the angular correlation pattern:

$$\Delta\theta = \omega\tau + \phi \qquad (1)$$

with

$$\omega = -g(\mu_N/\hbar)H_{\text{eff}} .$$

Here g is the nuclear g factor, $\mu_N/\hbar = 4.789 \times 10^3$ Hz/gauss, H_{eff} is the static magnetic field effective at the excited nucleus, τ is the nuclear mean lifetime, and ϕ is the transient field precession. ϕ/g can be calculated with the Lindhard-Winther model.[5]

Prior to this experiment, first-excited 2^+ state τ values were not available for all the Xe isotopes, but they could be conveniently measured concurrently with the angular shift. Preliminary values[6] of our results have been reported previously. Data for H_{eff} on xenon in iron exists, but there is evidence that the average value in an experiment of this nature (high energy implantation in the presence of an oxygen beam) may deviate considerably from the value obtained with samples prepared by other techniques.[7] On the assumption, supported by systematics, that the g factors do not vary much for a series of 2^+ levels of a given element, it is possible to extract H_{eff} and g_{av} from a series of angular shifts by a linear fit of the data to Eq. (1). Alternatively, if one g factor is independently measured, its value can be used to determine H_{eff}, and hence the remaining g factors. A recent radioactivity measurement for ^{132}Xe by deWaard, Kaufmann, and Rodgers[8] provided the calibration g factor for this experiment.

II. EXPERIMENTAL PROCEDURES

The first-excited 2^+ levels of the even xenon isotopes were populated by Coulomb excitation

using 36 and 42 MeV ^{16}O 5^+ beams generated by the Rutgers-Bell tandem Van de Graaff accelerator. Solid xenon targets with thicknesses in the range 0.5–1.5 mg/cm^2 were prepared by condensing Xe gas onto 10 mg/cm^2 natural Fe foils cooled to 4.2 K with liquid helium; the foils were cooled by means of a Cryotip refrigerator manufactured by the Air Products Corporation. Figure 1 shows the target chamber. The beam enters the chamber through the central hole of an annular Si surface-barrier detector and impinges on the target foil. This foil is soldered onto a copper ring with a 4-mm hole, which is rigidly fixed to the helium-cooled end of the Cryotip refrigerator. A magnetic field of 1.9 kOe is produced on the Fe foil by an electromagnet, the pole pieces of which are shown in the figure. The xenon gas to be frozen on the target enters the chamber through a 2-mm hole in a quartz nozzle that fits into the top of the bottom pole piece and extends close to the target foil through a hole in the heat shield. A thin layer of aluminum is evaporated on the nozzle to keep it from being charged by scattered beam particles.

The flow arrangement for the xenon gas is also shown in Fig. 1. A gas sample can be taken from a high pressure natural xenon gas bottle or from a low pressure xenon gas bottle, isotopically enriched[9] in ^{124}Xe-^{128}Xe, by opening the appropriate bottle into a short sampling tube, closed at the top by a valve. After closing the bottle valve, the sampling tube is opened into the previously evacuated gas line. Pressures in the gas line are typically 10–100 Torr for the natural gas and 0.2–2 Torr for the enriched gas.

After an oxygen beam is focused at the target and after the target has been cooled to liquid helium temperature, as indicated by a thermocouple reading, the needle valve in the xenon line is opened until solid xenon starts slowly forming on the target foil. This is immediately visible from the energy spectrum of oxygen ions backscattered at a mean angle of 168° into the annular Si detector. The thickness of the xenon layer can be deduced from the width of the energy distribution of these oxygen ions. An example of a particle spectrum is given in Fig. 2. Since the range of the xenon recoil nuclei in the solid layer is about 2.8 mg/cm^2, all recoiling nuclei are stopped in the iron backing. The efficiency of target formation turned out to be quite high, and it is estimated that only about 0.3 cm^3 of xenon gas (STP) is needed for one target of thickness 1 mg/cm^2.

In the course of a measurement, the energy distribution of the backscattered oxygen ions slowly broadens, indicating that the solid layer is becoming inhomogeneous. To form a new target the Cryotip is warmed up to about −50°C so that the xenon evaporates. This gas can be condensed in the recovery bottle so that very little is lost.

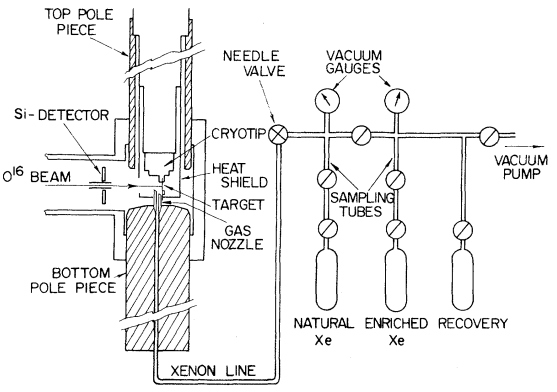

FIG. 1. Schematic view of target chamber and xenon line.

III. MEASUREMENTS

γ rays were observed, in coincidence with the particles backscattered from the Xe isotopes, by two Ge(Li) detectors in a horizontal plane containing the target. A 62-cm^3 detector was located 4.5 cm from the target at −67.5° with respect to the beam, while a 35-cm^3 detector was located 4.2 cm from the target at +45° with respect to the beam. Examples of the coincidence γ-ray spectra obtained with the 62-cm^3 detector for enriched and natural Xe targets are given in Figs. 3 and 4.

Standard fast-slow time-to-amplitude conversion (TAC) coincidence circuitry was used. The TAC

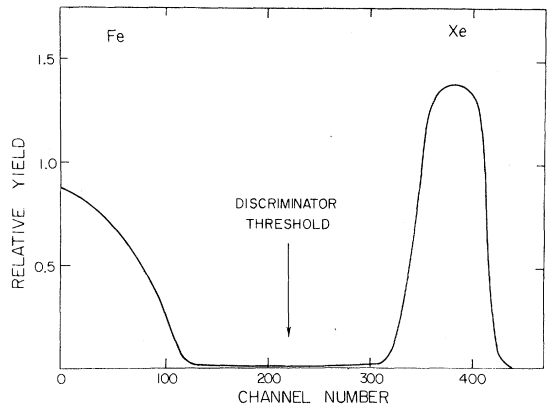

FIG. 2. Spectrum of ^{16}O particles backscattered from the target into the annular detector. The peak is due to ^{16}O scattered from the Xe layer while the low energy continuum is due to scattering from the Fe foil backing. The vertical arrow marks the discriminator threshold which triggers the slow-coincidence circuit.

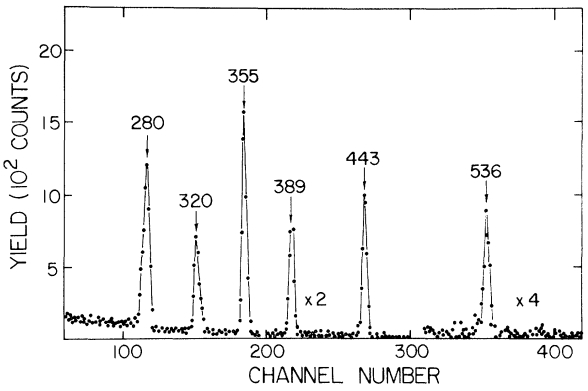

FIG. 3. An example of the γ-ray spectra obtained with the 62-cm^3 Ge(Li) detector in coincidence with backscattered particles lying above the discriminator level indicated in Fig. 2 when a xenon target enriched in ^{124}Xe is bombarded with 42-MeV ^{16}O ions. The γ rays at 355, 389, 443, and 536 keV result from the decay of the first-excited states of Xe isotopes with $A = 124$, 126, 128, and 130, respectively, while the lines at 280 and 320 keV result from the decay of levels in ^{129}Xe.

spectrum exhibited a peak with full width at half-maximum (FWHM) of 9 nsec for the 62-cm^3 detector and 7 nsec for the 35-cm^3 detector. Single-channel analyzer windows were set liberally around the TAC peak to insure that all true coincident events were recorded. In addition, all events from the particle detector above the discriminator threshold indicated in Fig. 2 were counted.

A. Reduced transition probabilities

Values for the reduced upward transition probability $B(E2; 0_1^+ \rightarrow 2_1^+)$ for the even xenon isotopes were derived from the Ge(Li) detector coincident γ-ray yields. The necessity for precise absolute target thickness and beam intensity values was circumvented by comparing the measured Rutherford scattering yield with the theoretical value. The yield of backscattered oxygen ions above the threshold indicated in Fig. 2 is due principally to elastic Rutherford scattering from the Xe nuclei. The maximum beam energy, 42 MeV, is only 67% of the Coulomb barrier for oxygen on ^{130}Xe.

For a given Xe isotope, the experimentally measured quantity is the ratio of the number of coincident photopeak γ rays produced from the decay of the first 2^+ level of that isotope as observed with the Ge(Li) detector to the number of elastically plus inelastically scattered particles observed with the particle detector. This ratio is related to the Coulomb-excitation cross section, which contains the reduced upward transition probability as a factor.

The absolute γ-ray photopeak detection efficiency

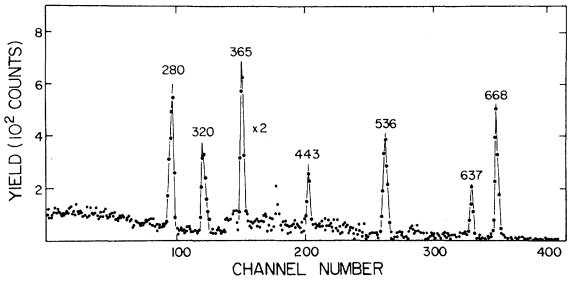

FIG. 4. Similar to Fig. 3, but for natural xenon. The γ rays at 443, 536, and 668 keV result from the decay of the first-excited states of Xe isotopes with $A = 128$, 130, and 132, respectively, while the lines at 280, 320, 365, and 637 keV result from the decay of levels in ^{129}Xe and ^{131}Xe.

was measured as a function of energy for both Ge(Li) detectors using a set of calibrated γ-ray sources placed in the same experimental geometry as used during the runs. The γ-ray angular correlation attenuation coefficients Q_2^γ and Q_4^γ for the Ge(Li) detectors were interpolated from the calculations of Camp and Van Lehn.[10] For the 62-cm^3 detector, these calculated values were checked by means of a measurement of the unperturbed particle-γ correlation following Coulomb excitation of the 2^+ first-excited state of ^{150}Sm. For this measurement, a target of 400 μg/cm^2 of ^{150}Sm was evaporated onto an 11.3 mg/cm^2 Cu foil and bombarded with a beam of 38-MeV ^{16}O ions. Copper was used as the host material since the particle-γ angular correlation for the decay of ^{150}Sm in Cu is known to be unperturbed.[11] The

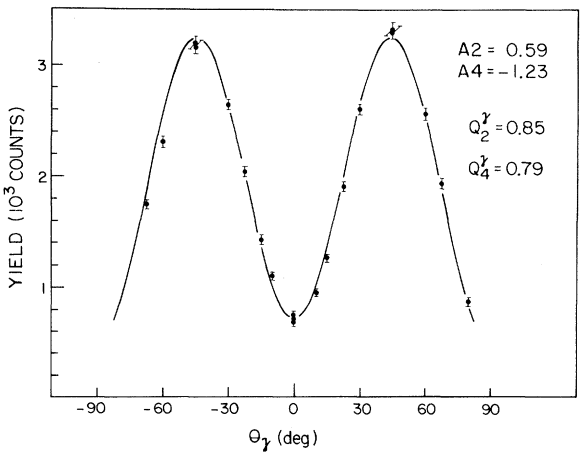

FIG. 5. The particle-γ angular correlation observed with the 62-cm^3 Ge(Li) detector in coincidence with backscattered ^{16}O particles when a ^{150}Sm target was bombarded with a beam of 38-MeV ^{16}O ions. The 334-keV 2^+ level of ^{150}Sm was excited by Coulomb excitation as the ^{150}Sm was recoil implanted into a Cu backing.

TABLE I. Summary of experimental results obtained for $\Delta\theta$ and $B(E2\uparrow)$ for $^{124-132}$Xe in iron. The g factors are obtained as discussed in the text. The results of other investigators are also included. Note that Ref. 21 does not quote an uncertainty for ^{128}Xe or ^{132}Xe. The numbers in parentheses indicate the uncertainty in the last decimal place. The lifetime values are based on the present measurements.

		$-\Delta\theta$ (mrad)		$B(E2\uparrow)$ (e^2b^2)			g factor		
A	2^+ energy (keV)	Present work	(Ref. 19)	Present work	Previous work	τ (psec)	Present work [a]	Present work [b]	(Ref. 19)
124	354.7	138 (9)		0.90 (7)		81 (7)	0.24 (5)	0.23 (2)	
126	388.5	116 (16)	89 (7)	0.79 (6)	0.77 (3) [c]	58 (5)	0.27 (6)	0.27 (4)	0.37 (7)
128	442.9	84 (5)	51 (2)	0.69 (5)	0.96 [d]	35 (3)	0.31 (6)	0.31 (3)	0.33 (7)
					0.70 (6) [e]				
130	536.1	31 (3)	32 (3)	1.00 (8)	0.69 (15) [d]	9.2 (7)	0.32 (7)	0.31 (4)	0.36 (7)
					0.61 (8) [e]				
					0.76 (20) [f]				
132	667.7	32 (3)	21 (3)	0.44 (3)	0.45 [d]	7.0 (6)	0.39 (5)	0.39 (5)	0.35 (5)
					0.32 (10) [g]				
					0.46 (5) [e]				

[a] Using $H_{\text{eff}} = 1.40 \pm 0.37$ MOe.
[b] Using $H_{\text{eff}} = 1.44 \pm 0.01$ MOe.
[c] Reference 20.
[d] Reference 21.
[e] Reference 22.
[f] Reference 23.
[g] Reference 24.

334-keV γ rays from the decay of the 2^+ ($\tau = 70$ psec) level were detected by the 62-cm^3 Ge(Li) detector in coincidence with the backscattered ^{16}O ions in essentially the same experimental geometry as used for the Xe runs, and at angles ranging from $-67.5°$ to $+80.0°$ with respect to the beam. The observed correlation for ^{150}Sm in Cu is shown in Fig. 5. From the best fit A_2 and A_4, and from the calculated particle angular-correlation attenuation coefficients Q_2^p and Q_4^p, the values of Q_2^γ and Q_4^γ were determined. The Q_2^γ determined in this way is about 7% smaller than the value calculated by Camp and Van Lehn,[10] while the Q_4^γ is about 8% larger than the calculated value. However, for the determination of $B(E2)$ values and of angular rotations, both sets of Q_2^γ and Q_4^γ lead to the same result within the experimental uncertainties. Therefore, for the 62-cm^3 detector the measured Q_2^γ and Q_4^γ were used, while for the 35-cm^3 detector the calculated values were used.

The particle detector angular correlation attenuation coefficients were calculated from the geometry employed using the formulation of Goldring, Kalish, and Spehl[12] and Yates.[13] The particle parameters for the particle-γ correlation were taken from Alder and Winther.[14]

The internal conversion coefficients used in the analysis were experimental values taken from the literature wherever possible[15]; when experimental values were not available, the theoretical values of Hager and Seltzer[16] were used. The correction for internal conversion was small; it varied from 2.4% (^{124}Xe) to 0.4% (^{132}Xe).

Since the peak in the particle spectrum contains elastically and inelastically scattered ^{16}O ions from all xenon isotopes, only a fraction of that observed peak is due to a particular isotope. The isotopic composition for the natural Xe targets was taken from the *Handbook of Chemistry and Physics* (51st edition), while the composition for the enriched Xe targets was assumed to be that quoted by the supplier. In addition, corrections to the elastic (Rutherford) scattering yield for inelastic (Coulomb excitation) scattering were made based on the transition rates found in the present work.

The Coulomb excitation cross sections were calculated using the symmetrized first order semiclassical theory of Alder *et al.*[14] and averaged over the solid angle subtended by the particle detector. The cross sections were also integrated over the target thickness, using the energy-loss tables of Northcliffe and Schilling[17] to estimate the energy loss of the beam as it traversed the target. The first-order calculations were checked using the Winther-de Boer multiple Coulomb excitation program[18] for the case of ^{132}Xe. Since the quadrupole moment of the first 2^+ state of ^{132}Xe, which enters in this program, has not been measured, it was estimated from the systematics of measured quadrupole moments of neighboring even-even nuclei. These more exact calculations differed by less than 3% from the first-order results; hence the first-order calculation was used throughout.

The measured $B(E2)$ values are given in Table I, along with the lifetimes deduced from our measurements. These are in reasonable agreement

with experimental values (Table I) from other investigations,[19-24] with the possible exception of ^{130}Xe where other investigators report longer lifetimes.

B. Angular rotations

In order to measure the rotation of the particle-γ angular correlation due to the effective hyperfine field on the implanted Xe atoms, the yield of coincident γ rays observed with the 62-cm^3 detector placed at $-67.5°$ with respect to the beam was measured as a function of the direction of the polarizing magnetic field. The Fe foil was polarized in a direction perpendicular to the beam axis and to the detection plane by application of an external 1.9 kOe field. The field direction was reversed periodically by computer control after observation of a preset number of backscattered particles above the discriminator level indicated in Fig. 2. The particle-γ angular correlation coefficients A_2 and A_4 were calculated as mentioned above. The observed γ-ray yields for field up and field down were corrected for random coincident events and for background.

The time resolution of the particle-γ coincidence circuitry resulted in the averaging of the observed correlations over excited-state lifetime. For the present experimental configuration, the time integral γ-ray angular correlation observed for nuclei precessing in a static magnetic field, oriented perpendicular to the beam axis and the plane defined by the detector geometry, is given by

$$W(\theta\updownarrow) = \sum_{k=0,2,4} b_k \frac{\cos(k\theta) \pm k\omega\tau \sin(k\theta)}{1+(k\omega\tau)^2}, \tag{2}$$

where

$$b_0 = 1 + \tfrac{1}{4}A_2 + \tfrac{9}{64}A_4,$$

$$b_2 = \tfrac{3}{4}A_2 + \tfrac{5}{16}A_4,$$

$$b_4 = \tfrac{35}{64}A_4,$$

and where ω is the Larmor precession frequency and τ is the mean life of the excited nuclear state. The arrows refer to the applied field direction.

Experimentally one measures the fractional change in γ-ray yield upon reversal of the magnetic field direction. This quantity is given by the relation

$$R = \frac{N\uparrow - N\downarrow}{N\uparrow + N\downarrow},$$

where $N\uparrow$ and $N\downarrow$ are the γ-ray yields for field up and down. Using the angular correlation function of Eq. (2), this ratio can also be written as

$$R = \frac{-2\omega\tau \sin 2\theta\{b_2/[1+4(\omega\tau)^2]\} + \{4b_4\cos 2\theta/[1+16(\omega\tau)^2]\}}{b_0 + \{b_2\cos 2\theta/[1+4(\omega\tau)^2]\} + \{b_4\cos 4\theta/[1+16(\omega\tau)^2]\}}, \tag{3}$$

where $\omega\tau$ is the angular rotation of the correlation. Since Eq. (3) does not have a closed-form solution for $\omega\tau$, an iterative technique is used to find the value of $\omega\tau$ which satisfies the relation. The observed angular rotations $\Delta\theta_{\text{exp}}$ for the Xe isotopes implanted in an Fe host are given in Table I. In addition, these rotations are plotted in Fig. 6 as a function of mean life. Also included in Table I are angular rotations for $^{126-132}$Xe obtained by Norlin *et al.*[19]

IV. ANALYSIS OF THE MEASURED ANGULAR ROTATIONS

Previous work[4] has shown that excited nuclei recoil implanted into a polarized ferromagnetic host interact with both static and dynamic hyperfine magnetic fields. The static hyperfine magnetic interaction occurs after the recoiling ion stops. The dynamic hyperfine magnetic interaction occurs while the recoiling ions slow down in the ferromagnetic host prior to stopping. This field arises from interaction of the magnetic moments of recoil nuclei with polarized electrons in the stopping medium and causes an "impulse" precession ϕ of the angular correlation pattern. Lindhard and Winther[5] have proposed a scattering model which relates the strength of this transient interaction to an enhancement of the polarized free electron density at the recoiling nuclei. The Coulomb scattering of polarized electrons gives rise to a magnetization density proportional to the polarized electron density, resulting in a magnetic field at the scattering center via the Fermi contact interaction. The Lindhard-Winther model is in agreement with the presently available experimental results,[7] for $Z > 10$, and has been used in this work to estimate the size of the γ-ray angular precession induced by the transient field interaction.

It is convenient to write the measured precession angle $\Delta\theta$, given by Eq. (1), as

$$\Delta\theta = -g(\phi/g) - g\frac{\mu_N}{\hbar}H_{\text{eff}}\tau, \tag{4}$$

where ϕ/g is the reduced transient field precession angle and H_{eff} is the effective static hyperfine magnetic field. The Lindhard-Winther theory

for the transient field interaction gives the effective magnetic field at a recoiling nucleus as a function of its velocity. The reduced precession angles (ϕ/g) were calculated using a computer program to numerically integrate the derived transient magnetic field over the velocity range of the recoiling nuclei using the energy-loss theory of Lindhard, Scharff, and Schiøtt.[25] This calculation yields $\phi/g = -36 \pm 6$ mrad for the Xe isotopes, the uncertainty including the slight dependence on mean life.

In order to extract the hyperfine magnetic field and g-factor values from the observed angular rotations and the reduced transient field rotation, at least one 2^+ state g factor must be known beforehand. The g factor of the 668-keV 2^+ state in ^{132}Xe has been measured recently by deWaard, Kaufmann, and Rodgers.[8] These authors performed a perturbed angular correlation measurement on the 772-668 keV γ-γ cascade in ^{132}Xe, emitted in the decay of a ^{132}Te source implanted in iron. ^{132}Xe granddaughter nuclei were assumed to be in equivalent sites to Te in iron and to experience a field $H_{hf} = 1440 \pm 10$ kOe, as deduced from recent Mössbauer-effect measurements.[26] The PAC measurements yielded a rotation $\omega\tau = -19.2 \pm 2.1$ mrad which, combined with the lifetime $\tau = 7.0 \pm 0.6$ psec found in the present investigation, yields $g(668\ \text{keV}) = 0.39 \pm 0.05$.

Combining the above lifetime and g factor with the observed angular rotation and transient field result for the ^{132}Xe 2_1^+ state, one obtains for the magnetic hyperfine field experienced by Xe atoms implanted in Fe the value

$$H_{eff} = +(1.40 \pm 0.37) \times 10^6 \text{ Oe}.$$

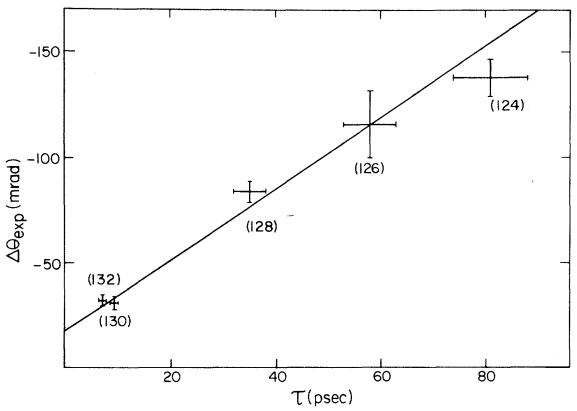

FIG. 6. The observed angular rotation $\Delta\theta$ versus mean lifetime τ for the 2^+ first-excited states of the even Xe isotopes implanted into Fe. The number in parenthesis is the atomic mass number of the Xe isotopes. The solid line is a fit to the data of the form $-\Delta\theta = a + b\tau$.

The large uncertainty is due to the comparable values of ϕ and $\Delta\theta$ in this case. This value agrees with the more precise results of the Mössbauer-effect experiments[26] for an equivalent dilute substitutional xenon in iron sample. We have used $H_{eff} = 1.44 \pm 0.01$ MOe to extract g factors for the other Xe isotopes. The justification for using this value is discussed in Sec. V A. The g factors are given in Table I along with the results quoted by Norlin *et al.*[19] for $^{126\text{-}132}$Xe. The largest difference (though still within quoted uncertainties) is for ^{126}Xe, where the Norlin value is from a more difficult γ-γ radioactivity experiment. The ^{130}Xe results would show a larger difference [0.31(4) vs 0.47(9)] if the Norlin value were recalculated with the lifetime obtained in our measurements. The uncertainties quoted for g reflect the uncertainties in $\Delta\theta$, the calculated ϕ/g, τ, and H_{eff} from Ref. 26. Table I also presents g factors (and uncertainties) extracted using the less precise value for H_{eff} obtained from the ^{132}Xe measurement.

V. DISCUSSION

A. Hyperfine fields

The study of hyperfine fields on dilute impurities in ferromagnetic hosts is an interesting and important area of hyperfine interaction physics.[27] The case of xenon in iron is especially intriguing and has been the subject of several previous investigations.[26,28] In addition, the problem of xenon radiation damage and lattice location is of importance to reactor technology because of the high xenon yield from uranium fission.

Nuclear orientation experiments[29] on xenon implanted into iron yielded $H_{eff} \approx 1.5$ MOe for about 50% of the implanted nuclei. The remaining xenon experienced considerably reduced fields which could not be clearly determined. Subsequent Mössbauer-effect experiments[26] showed that, indeed, there existed several sites for the implanted xenon, with corresponding hyperfine fields, the maximum value being 1.44 ± 0.01 MOe. The fraction of nuclei experiencing the maximum field was a function of the implantation procedure, total dose, and sample temperature history. Channeling studies indicated that the maximum field could be correlated with a substitutional site in a local damage-free region.[30] Groups at Groningen, Leuven, and Bell Laboratories have continued to study the Xe system. Their results indicate the existence of a second high field, ≈1.1 MOe, (which may be associated with substitutional Xe having a nearest-neighbor vacancy) and a low field (presumably due to extended xenon-vacancy clusters). Studies at Leuven[26] indicate that high field sites

TABLE II. Theoretical results for $^{124-132}$Xe 2^+ state parameters measured. See text for a discussion of the individual calculations. Present experimental results are included for comparison.

	$B(E2; 0_1^+ \rightarrow 2_1^+)$ $(e^2\,b^2)$						g factor			
A	Exp.	Single-particle estimate [a]	Ref. 42	Ref. 43	Ref. 44	Ref. 46	Exp.	Ref. 41	Ref. 47	Hydrodynamic model [b]
124	0.90 (7)	1.8×10^{-2}	···	···	···	0.99 (14)	0.23 (2)	···	0.36	0.44
126	0.79 (6)	1.9×10^{-2}	1.08	0.35	···	···	0.27 (4)	0.26	0.36	0.43
128	0.69 (5)	1.9×10^{-2}	0.88	0.18	···	···	0.31 (3)	0.25	0.35	0.42
130	1.00 (8)	2.0×10^{-2}	0.76	0.24	···	···	0.31 (4)	0.28	0.34	0.42
132	0.44 (3)	2.0×10^{-2}	0.59	0.16	0.61	···	0.39 (5)	0.33	0.34	0.41

[a] S. J. Skorka, J. Hertel, and T. W. Retz-Schmidt, Nucl. Data A2, 347 (1966).
[b] $g = Z/A$.

are favored at low doses.

In the present recoil-implantation experiments, the *a priori* expectation was for high-field sites. The reasons for this expectation were threefold: (1) the kinematics of the Xe-Fe slowing down favors replacement collisions; (2) recoil implantation yields very dilute samples; and (3) at the low temperature at which these experiments were carried out, radiation damage (vacancies and interstitials) should be relatively immobile and unable to migrate to the impurity site. The latter effect coupled with the low beam current used should also inhibit primary beam radiation damage as discussed by Hubler and Murnick.[31]

The result extracted from our data for H_{eff} (1.40 ± 0.37 MOe) is entirely consistent with the above discussion and serves to reinforce the hypothesis discussed. Future similar experiments, especially with krypton, should also yield interesting hyperfine field information.

The Uppsala group has performed similar experiments to ours and obtained a smaller effective hyperfine field.[19] The major difference between the experiments was that the Uppsala work was performed at room temperature utilizing ion-implanted targets. Such an experiment is subject to higher xenon concentrations at the recoil site due to diffusion, room temperature damage migration, and primary beam radiation damage because of the higher beam currents necessary with thin implanted samples.

B. Nuclear properties of the even xenon isotopes

The even xenon isotopes are in a region of nearly spherical nuclei with a structure of low-lying levels that may be described by the collective vibrational model. With a pure vibrational model, one expects a 0_1^+ ground state, a (one-phonon) 2_1^+ first-excited state, and a (two-phonon) triplet of levels 0_2^+, 2_2^+, and 4_1^+ at twice the energy of the first 2^+ state. The theory predicts that the decay of the first excited state is a strongly enhanced $E2$ transition. The stopover transition $(2_2^+ \rightarrow 2_1^+)$ from the second 2^+ state is a pure $E2$ transition (since magnetic transitions are forbidden) and the crossover transition $(2_2^+ \rightarrow 0_1^+)$ is forbidden.

For the even xenon isotopes the expected 0_2^+ state has not been observed, but the 2_2^+ and 4_1^+ states lie at the right excitation energies; the ratio of the excitation energies of the second 2^+ to the first 2^+ levels is $E(2_2^+)/E(2_1^+) = 2.1 \pm 0.2$ for the even xenon nuclei in the mass range $A = 124$–132.[32] Moreover, the $2_1^+ \rightarrow 0_1^+$ transition strengths are strongly enhanced over the single-particle estimates (see Table II). While the lifetimes of the second 2^+ states have not been determined, the measured branching and mixing ratios [33-38] for the decay of these levels indicate that the $2_2^+ \rightarrow 2_1^+$ transitions are primarily $E2$ $[\delta(E2/M1) > +5]$ and that the crossover transitions $2_2^+ \rightarrow 0_1^+$ are greatly inhibited; as an example,[38] for ^{130}Xe $B(E2; 2_2^+ \rightarrow 0_1^+)/B(E2; 2_2^+ \rightarrow 2_1^+) = 0.0064 \pm 0.0005$, assuming both transitions are pure $E2$.

In addition to the vibrational model above, one may also describe the levels of these nuclei in terms of the collective rotational model. Morinaga and Lark[39] classified several of the low-lying levels of the even xenon isotopes in the mass range $A = 122$–136 into ground-state rotational bands up to spin 10^+, while Sakai[40] has classified these levels into quasi-ground, quasi-β, and quasi-γ bands, and has discussed the interband transition strengths in terms of the band-mixing parameter.

Several authors have attempted to treat the even-even spherical nuclei in more detail than is used in the simple collective vibrational model mentioned above. Kisslinger and Sorensen[41] have used the pairing-plus-quadrupole model employing the quasiparticle random phase approximation (QRPA) to calculate energy levels, transition strengths, and static electromagnetic moments for a wide range of spherical nuclei, including

the Xe isotopes. Their results for the g factors for the 2_1^+ states of the Xe isotopes studied in the present work are given in Table II, and are in agreement with our observations; the theory accurately predicts the lowering of the g factors from the hydrodynamical prediction $g_{2+} = Z/A$.

Uher and Sorensen[42] have improved upon the earlier work of Kisslinger and Sorensen[41] by including more single-particle levels in their calculation. They have used an effective quadrupole charge parameter $\epsilon_{\text{eff}} = 0.3e$ to compensate for levels not included in the calculation, and have predicted $B(E2\uparrow)$ for $^{126-136}$Xe. These values are included in Table II and are about 30% larger than the present results except for the case of ^{130}Xe, where their prediction is about 25% smaller than our observation.

Almoney and Borse[43] used the pairing-plus-quadrupole Hamiltonian but retained the single quasiparticle terms to produce anharmonic effects in a wide range of spherical nuclei. They calculated quadrupole moments and $B(E2\uparrow)$ values for the first 2^+ states of several Xe isotopes. Their results are also presented in Table II. The calculations lead to nonzero values of the static quadrupole moment of the first 2^+ state and of the crossover $B(E2; 0_1^+ \rightarrow 2_2^+)$ that are qualitatively correct for other spherical nuclei, but the values found for $B(E2; 0_1^+ \rightarrow 2_1^+)$ of the Xe isotopes are smaller than the experimental values by a factor of 3.

Goswami and Lin[44] have used the surface δ interaction[45] (SDI) and the QRPA to calculate $E2$ transition strengths from the one phonon 2_1^+ state to the ground state for several doubly open-shell vibrational nuclei including ^{132}Xe and ^{134}Xe. Shell model states for both neutrons and protons include the $2d_{5/2}$, $1g_{7/2}$, $1h_{11/2}$, $3s_{1/2}$, and $2d_{3/2}$ orbitals, and the authors used effective charges $\epsilon_p = 1.76$ and $\epsilon_n = 0.76$. Their result for ^{132}Xe, given in Table II, is about 40% greater than the present experimental result.

Ross and Bhaduri[46] have developed a simple semiempirical formula to relate the $E2$ transition strengths between ground and 2_1^+ states for neighboring doubly even nuclides. Using a difference equation approach, they have predicted a $B(E2; 0_1^+ \rightarrow 2_1^+)$ value for ^{124}Xe in agreement with the present experimental result.

Greiner[47] has used the hydrodynamical rotation-vibration model but uses the fact that the pairing force G_p between protons is stronger than the pairing force G_n between neutrons. Thus, the neutron distribution is more deformed than the proton distribution, which leads to a lowering of the g factor for these states from the hydrodynamical Z/A value. Greiner's results are given in Table II; while his values are in agreement with the present work for $^{128-132}$Xe, they show the opposite dependence on mass number from that observed experimentally. That is, the measured g factors increase monotonically with A, while the theory predicts monotonically decreasing values.

VI. SUMMARY

A systematic study of first 2^+ levels of $^{124-132}$Xe has yielded $B(E2\uparrow)$ and g factors in reasonable agreement with microscopic nuclear structure calculations. In order to further understand the structure of these even-even nuclei, more experimental information is necessary. In particular, experimental values for lifetimes and mixing ratios for the decays of the higher excited states are vital for the understanding of the rotational or vibrational character of these nuclei. In addition, extension of the present measurements to ^{136}Xe to study the effects of closing the $h_{11/2}$ neutron shell is desirable. The ^{136}Xe experiment is more difficult than the present studies because of the high 2_1^+ state energy (1.32 MeV) and the resulting low Coulomb excitation cross section.

The method of solid target preparation at 4 K enabled the large hyperfine field effective on Xe in iron to be used for these studies. This target preparation technique is clearly applicable to similar experiments with other normally gaseous elements. Our results are consistent with low temperature, short time extrapolations from detailed Mössbauer-effect studies of the xenon implanted into iron system.

---

*Present address: State University of New York at Stony Brook, Stony Brook, New York 11794.
†Present address: University of California, Los Angeles, California 90024.
‡Work supported in part by the National Science Foundation.
§Present address: Natuurkundig Laboratorium, Groningen, Netherlands.
¶Associate of the Graduate Faculty, Rutgers University, New Brunswick, New Jersey 08903.

[1] R. R. Borchers, in *Hyperfine Interactions in Excited Nuclei*, edited by G. Goldring and R. Kalish (Gordon and Breach, New York, 1971), p. 31.
[2] G. M. Heestand, R. R. Borchers, B. Herskind, L. Grodzins, R. Kalish, and D. E. Murnick, Nucl. Phys. A133, 310 (1969).
[3] H. W. Kugel, T. Polga, R. Kalish, and R. R. Borchers, Phys. Lett. 32B, 463 (1970).

[4]R. R. Borchers, B. Herskind, J. Bronson, L. Grodzins, R. Kalish, and D. Murnick, Phys. Rev. Lett. 20, 424 (1968).
[5]J. Lindhard and A. Winther, Nucl. Phys. A166, 413 (1971).
[6]D. Gordon, L. Eytel, H. deWaard, E. N. Kaufmann, and D. Murnick, in *Proceedings of the International Conference on Nuclear Physics*, edited by J. de Boer and H. J. Mang (North-Holland, Amsterdam/American Elsevier, New York, 1973), Vol. 1, p. 259.
[7]G. K. Hubler, H. W. Kugel, and D. E. Murnick, Phys. Rev. C 9, 1954 (1974).
[8]H. deWaard, E. N. Kaufmann, and J. W. Rodgers, Z. Phys. 264, 423 (1973).
[9]Mound Laboratory, Monsanto Research Corporation, Miamisburg, Ohio.
[10]D. C. Camp and A. L. Van Lehn, Nucl. Instrum. Methods 76, 192 (1969).
[11]D. E. Murnick, J. D. Bronson, B. Herskind, R. R. Borchers, and L. Grodzins, Phys. Rev. 163, 254 (1967).
[12]G. Goldring, R. Kalish, and H. Spehl, Nucl. Phys. 80, 33 (1966).
[13]M. J. L. Yates, in *Perturbed Angular Correlations*, edited by E. Karlsson, E. Matthias, and K. Siegbahn (North-Holland, Amsterdam, 1964), p. 453.
[14]K. Alder and A. Winther, K. Dan. Vidensk. Selsk. Mat.-Fys. Medd. 31, No. 1 (1956); K. Alder, A. Bohr, T. Haus, B. Mottelson, and A. Winther, Rev. Mod. Phys. 28, 432 (1956).
[15]H. K. Carter, J. H. Hamilton, J. C. Manthuruthil, S. R. Amtey, J. J. Pinajian, and E. F. Zganjar, Phys. Rev. C 1, 649 (1970); H. W. Boyd and J. H. Hamilton, Nucl. Phys. 72, 604 (1965).
[16]R. S. Hager and E. C. Seltzer, Nucl. Data A4, 1 (1968).
[17]L. C. Northcliffe and R. F. Schilling, Nucl. Data A7, 233 (1970).
[18]A. Winther and J. de Boer, in *Coulomb Excitation* (Academic, New York, 1966), p. 303 [California Institute of Technology, Technical Report, 1965 (unpublished)].
[19]L.-O. Norlin, K. Johansson, E. Karlsson, and S. Ogaza, in Proceedings of the International Conference on Hyperfine Interactions Studied in Nuclear Reactions and Decay, Uppsala, Sweden, 1974 (unpublished), p. 118.
[20]T. J. de Boer, E. W. Ten Napel, and J. Blok, Physica (Utr.) 29, 1013 (1963).
[21]P. F. Kenealy, G. B. Beard, and K. Parsons, Phys. Rev. C 2, 2009 (1970); G. F. Pieper, C. E. Anderson, and N. P. Heydenburg, Bull. Am. Phys. Soc. 3, 38 (1958).
[22]L. O. Edwardsson and L. O. Norlin (unpublished).
[23]J. Burde, S. Eshhar, A. Ginzburg, and E. Navon, Nucl. Phys. A229, 387 (1974).
[24]W. D. Hamilton, Proc. Phys. Soc. Lond. 78, 1064 (1961).
[25]J. Lindhard, M. Scharff, and H. E. Schiøtt, K. Dan. Vidensk. Selsk. Mat.-Fys. Medd. 33, No. 14 (1963).
[26]M. van Rossum, G. Langouche, H. Patlyn, G. Dumond, J. Odeurs, A. Meykens, R. Coussement, and P. Boolchand, in Proceedings of Magnetism Conference, 1975 (American Institute of Physics, New York, to be published); H. deWaard, R. L. Cohen, S. R. Reintsema, and S. A. Drentje, Phys. Rev. B 10, 3760 (1974).
[27]See, for example, Proceedings of the International Conference on Hyperfine Interactions Studied in Nuclear Reactions and Decay, Phys. Scr. (to be published).
[28]H. deWaard and L. C. Feldman, in *Applications of Ion Beams to Metals*, edited by S. T. Picraux (Plenum, New York, 1974), and references therein.
[29]R. E. Silverans, R. Coussement, H. Patlyn, E. Schoeters, and L. Vanneste, Z. Phys. 267, 145 (1974).
[30]L. C. Feldman and D. E. Murnick, Phys. Rev. B 5, 1 (1972).
[31]G. K. Hubler and D. E. Murnick, in Proceedings of the International Conference on Hyperfine Interactions Studied in Nuclear Reactions and Decay, Uppsala, Sweden, 1974 (unpublished), p. 66; G. K. Hubler, Ph.D. thesis, Rutgers University, 1972 (unpublished).
[32]R. L. Auble, Nucl. Data Sheets 9, 125, 157 (1973); F. E. Bertrand, *ibid.* 10, 91 (1973); H. R. Hiddleston and C. P. Browne, *ibid.* 13, 133 (1974); *Nuclear Level Schemes A=45 through A=257 from Nuclear Data Sheets*, edited by D. J. Horen *et al.* (Academic, New York, 1973).
[33]K. S. Krane and R. M. Steffen, Phys. Rev. C 4, 1419 (1971); K. S. Krane, C. E. Olsen, and W. A. Steyert, *ibid.* 5, 1671 (1972).
[34]H. W. Taylor and B. Singh, Can. J. Phys. 49, 2724 (1971); B. Singh and H. W. Taylor, Nucl. Phys. A147, 12 (1970).
[35]J. H. Hamilton, H. K. Carter, and J. J. Pinajian, Phys. Rev. C 1, 666 (1970).
[36]P. K. Hopke, A. G. Jones, W. B. Walters, A. Prindle, and R. A. Meyer, Phys. Rev. C 8, 745 (1973); R. A. Meyer and W. B. Walters, *ibid.* 9, 2379 (1974).
[37]S. M. Qaim, Nucl. Phys. A154, 145 (1970).
[38]W. Gelletly, W. R. Kane, and D. R. MacKenzie, Phys. Rev. C 9, 2363 (1974).
[39]H. Morinaga and N. L. Lark, Nucl. Phys. 67, 315 (1965).
[40]M. Sakai, Nucl. Data A10, 511 (1972); M. Sakai (private communication).
[41]L. S. Kisslinger and R. A. Sorensen, Rev. Mod. Phys. 35, 853 (1963).
[42]R. A. Uher and R. A. Sorensen, Nucl. Phys. 86, 1 (1966).
[43]S. R. Almoney and G. J. Borse, Nucl. Phys. A171, 660 (1971).
[44]A. Goswami and L. Lin, Nucl. Phys. A186, 88 (1972).
[45]R. Arvieu and S. A. Moszkowski, Phys. Rev. 145, 830 (1966).
[46]C. K. Ross and R. K. Bhaduri, Nucl. Phys. A196, 369 (1972).
[47]W. Greiner, Nucl. Phys. 80, 417 (1966).